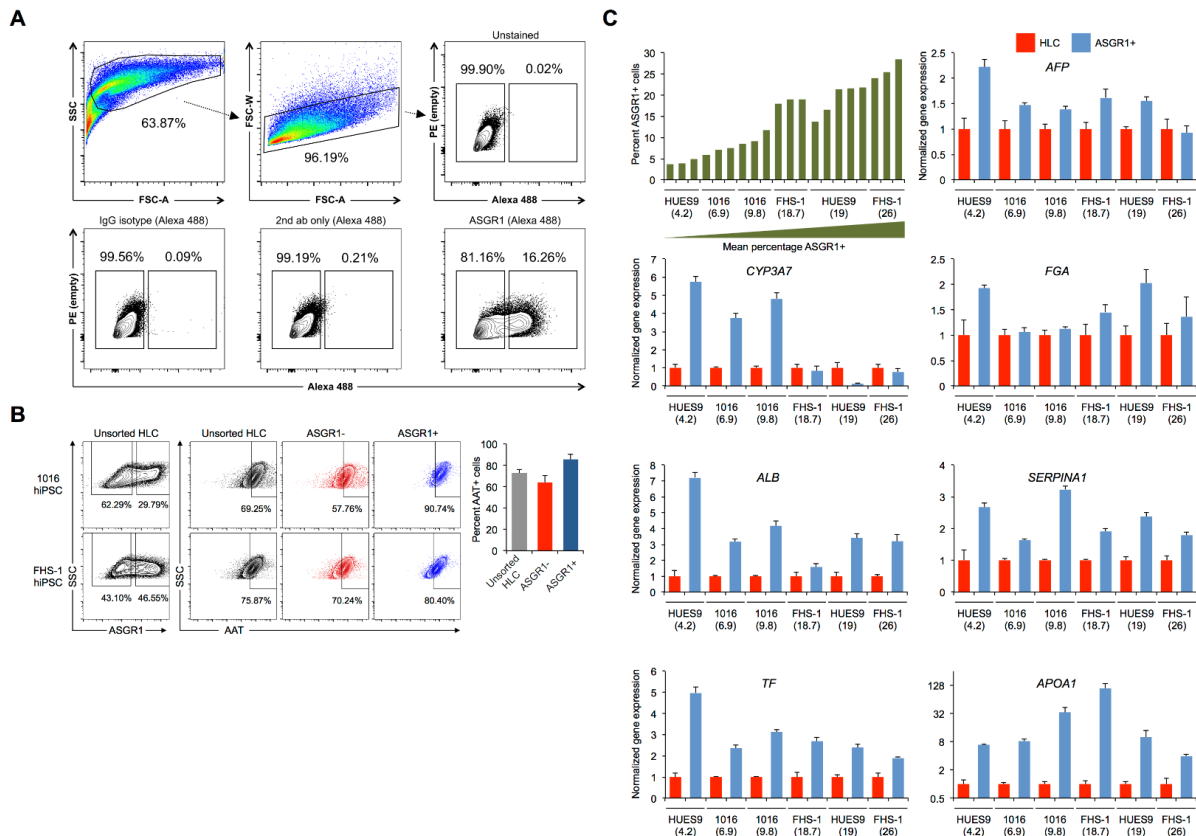


**Figure S1. Flow cytometry analysis of HLC differentiation, related to Figure 1.** (A) Gating used for flow cytometry analyses; single cells were defined by FSC-A/SSC (cell size and granularity) and FSC-W (cell width) to exclude debris, cell clumps, and doublets. (B) Albumin and ASGR1 expression after the IMH differentiation stage with corresponding staining controls. Alexa 488 and Alexa 594 conjugated secondary antibodies were used with albumin and ASGR1 primary antibodies respectively; gating for albumin and ASGR1 positive cells was performed using secondary-only and isotype-control staining conditions

respectively. (C) Albumin and ASGR1 expression after the MH differentiation stage with corresponding staining controls. Alexa 647 and Alexa 594 conjugated secondary antibodies were used with albumin and ASGR1 primary antibodies respectively; gating for albumin and ASGR1 positive cells was performed using secondary-only and isotype-control staining conditions respectively. A secondary-only staining control is also shown for ASGR1. (D) Kinetics of albumin and ASGR1 expression during the final stages of HLC differentiation as determined by intracellular flow cytometry. Shown are mean percent positive cells at the IMH and MH stages based on multiple independent differentiations ( $n = 5 - 15$  replicates per marker, per stage). Error bars represent s.e.m. Asterisks indicate statistically significant differences in mean percentage of positive cells at the IMH and MH stages for each marker by Student's  $t$ -test. \*,  $P < 0.05$ . (E) Flow cytometry analysis of ASGR1 and HNF4A co-expression with staining controls. Alexa 594 and Alexa 488 conjugated secondary antibodies were used for ASGR1 and HNF4A staining respectively. Gating was performed based on secondary-only (fluorescence minus one) staining conditions. (F) Flow cytometry analysis of ASGR1 and albumin co-expression with staining controls. Alexa 594 and Alexa 488 conjugated secondary antibodies were used for ASGR1 and albumin staining respectively. Gating for ASGR1 and albumin positive cells was performed based on isotype-control and secondary-only staining conditions respectively. (G-H) Efficiency of HLC differentiation with four different hPSC lines over multiple independent experiments. Shown are percent albumin-positive (G) and surface ASGR1-positive (H) cells determined by flow cytometry analysis after the MH differentiation stage, illustrating a range of differentiation efficiencies.



**Figure S2. Detailed results of ASGR1 FACS and hepatocyte marker gene expression analysis, related to Figure 2.** (A) Strategy and staining controls for FACS isolation of ASGR1+ HLCs. Shown are results of a representative differentiation and FACS experiment. (B) Left: two different hPSC lines were differentiated to HLCs. The percentage of cells expressing the hepatocyte marker alpha-1 antitrypsin (AAT) among unsorted HLCs, surface ASGR1-negative cells, and surface ASGR1-positive cells was quantified by intracellular flow cytometry. Right: mean percent AAT-positive cells by flow cytometry, among unsorted HLCs, surface ASGR1-negative cells, and surface ASGR1-positive cells ( $n = 2$  differentiations). Error bars represent s.e.m. (C) ASGR1 FACS and hepatocyte marker gene expression analysis by qRT-PCR. Gene expression data is displayed as a heatmap in Figure 2C. Three different hPSC lines were differentiated to HLCs, with two independent differentiations performed per cell line (differentiations performed in triplicate or greater,  $n = 6 - 8$  biological replicates per cell line). Data are arranged according to mean percent ASGR1+ cells obtained in each differentiation. Green bars: percentage surface ASGR1+ cells after the MH

differentiation stage. All other graphs show qRT-PCR gene expression analysis in unsorted HLCs (“HLC,” red bars) and ASGR1+ cells (“ASGR1+,” blue bars) isolated by FACS. Expression levels are relative to *RPLP0* expression; gene expression levels in ASGR1+ cells were normalized to level in unsorted HLCs. Shown are normalized mean expression levels for each differentiation ( $n = 3 - 5$  paired biological replicates per differentiation). Error bars represent s.e.m.

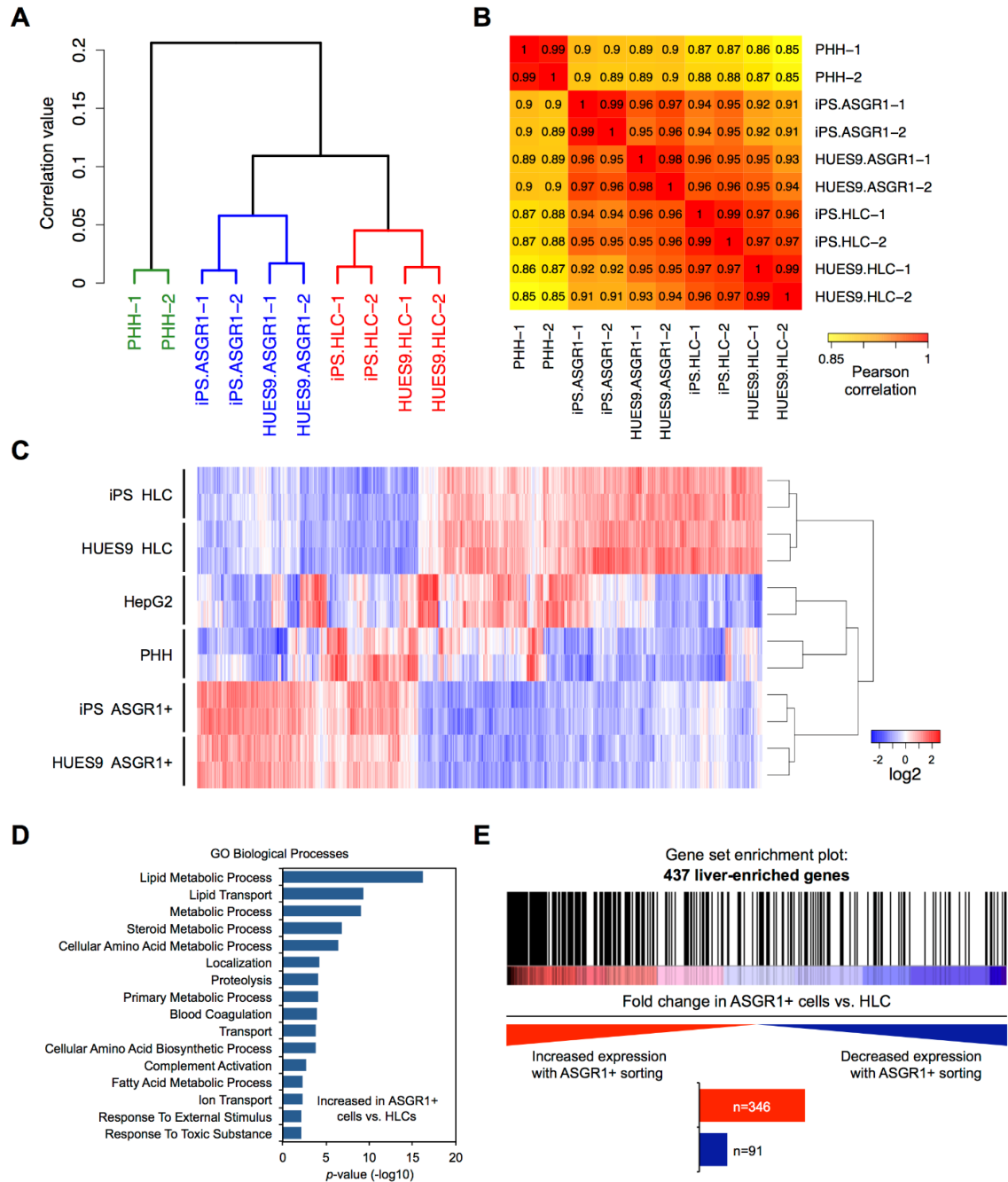


**Figure S3. Additional analyses of microarray gene expression profiling data from ASGR1-positive cells, unsorted HLCs, primary human hepatocytes, and HepG2 hepatoma cells, related to figure 3. (A) Hierarchical clustering of ASGR1-positive, HLC, and PHH samples based on all genes measured by transcriptional microarray and expressed above background. (B) Heatmap showing pairwise Pearson correlation values for ASGR1-**

positive, HLC, and PHH samples based on the same expression data used in part A. Yellow, orange, and red color denotes lower, intermediate, and higher correlation respectively. (C) Heatmap of hierarchical clustering performed on all genes differentially expressed between ASGR1-positive cells and HLCs at a 5% FDR. Blue, below average expression, red, above average expression. 813 probesets differentially expressed between ASGR1+ and unsorted HLC at 5% FDR; 318 upregulated and 495 downregulated in ASGR1+ vs. unsorted HLCs respectively. (D) Functional enrichment analysis of genes differentially expressed in ASGR1-positive cells relative to HLCs. (E) Gene set enrichment analysis (GSEA). Microarray gene expression data was arranged based on greater average expression in ASGR1-positive cells (red color) or unsorted HLCs (blue color). Vertical black bars represent genes within the liver-enriched gene set.

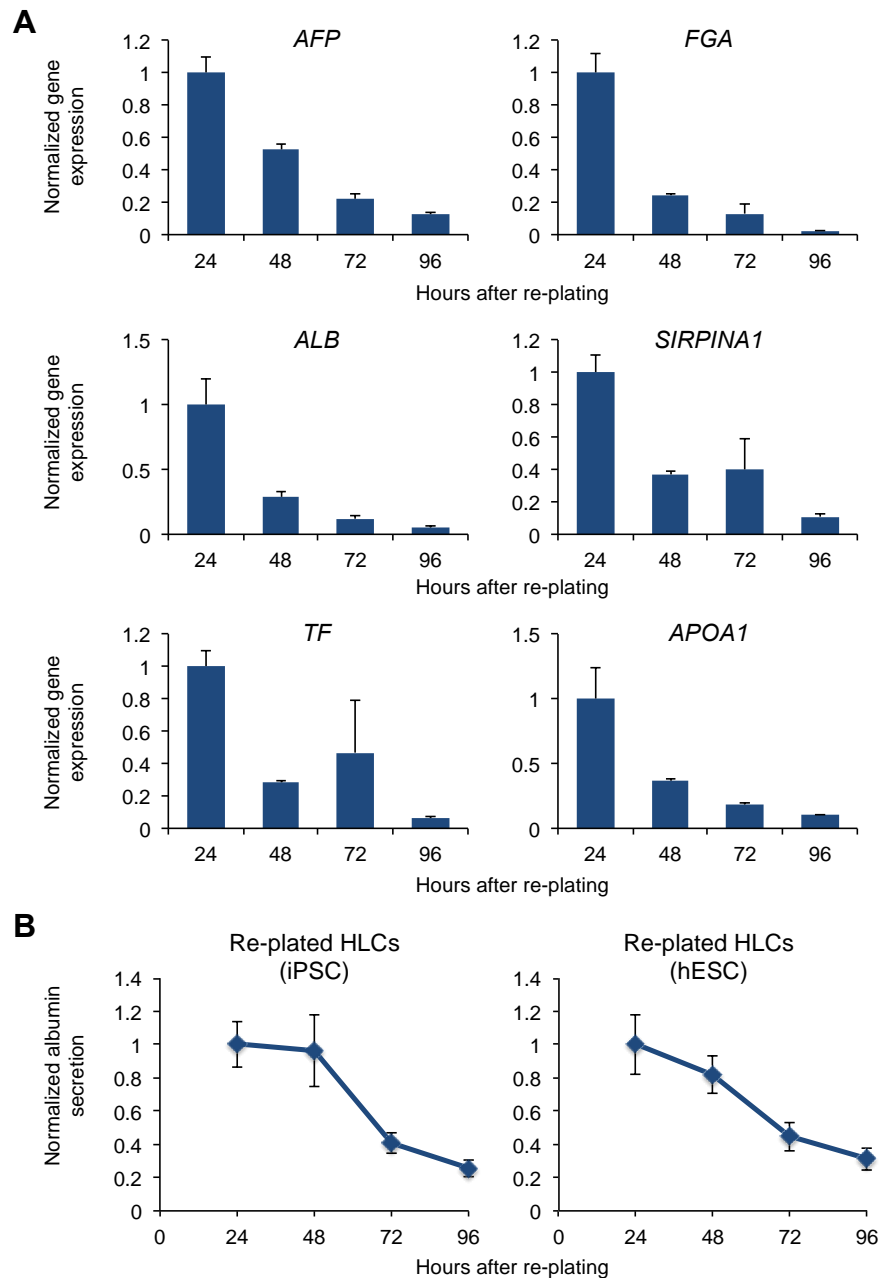


**Figure S4. Hepatocyte marker gene expression and albumin secretion declines as anticipated following re-plating of ASGR1 MACS-enriched HLCs.** (A) Changes in hepatocyte marker gene expression over time were determined by qRT-PCR after re-plating HLCs differentiated from a representative hESC line. Gene expression levels were calculated relative to *RPLP0* expression and normalized to gene expression level at 24 hours post re-plating for each gene ( $n = 3$  differentiation wells per time point). Error bars represent s.e.m. (B)

Quantification of albumin secretion by ELISA following re-plating of HLCs differentiated from two hPSC lines. Albumin concentration at the indicated time points were calculated using a standard curve and normalized to the level at 24 hours post re-plating for each cell line ( $n = 3$  differentiation wells per cell line, per time point). Medium was collected after 24 hours in culture for each time point. Error bars represent s.e.m.



**Table S1. Distribution of liver-enriched genes in gene set enrichment analysis (GSEA) comparing ASGR1+ cells and unsorted HLCs, related to Figure S3E.**

Subset of liver-enriched genes with greater expression in ASGR1+ cells. 205 genes contributed most strongly to the enrichment result (core enrichment). 346 of 437 genes had greater expression in ASGR1+ cells vs. unsorted HLCs.						Liver-enriched genes with lower expression in ASGR1+ cells. 91 of 437 genes had lower expression in ASGR1+ cells vs. unsorted HLCs		
AADAC	ASGR1	FBP1	LEPR	SEPHS2	TTR	ABCB4	FMO4	SEC14L2
ABCG8	ASGR2	FETUB	LIPC	SERPINA10	UGT2B4	ABCG5	GCGR	SEC14L4
ACAA1	ASS1	FGA	MAT1A	SERPINA4	UGT3A1	ACAT2	GHR	SLCO1B1
ACAA2	ATF5	FGB	METTL7B	SERPINA6	VTN	ACOT12	GLS2	SOD1
ACADSB	AZGP1	FGFR4	MTHFS	SERPINA7	ZNHIT1	ANXA10	GLT1D1	SPP2
ACAT1	BAAT	FGG	MTTP	SERPINC1		APOC4	GNE	STEAP3
ACMSD	BPHL	FGL1	MUT	SERPIND1		AQP9	GNPNAT1	THPO
ACOX1	BRP44	FMO5	NAT8	SERPINF2		AS3MT	GPR126	TNFSF14
ACOX2	C1S	G6PC	NEK6	SERPING1		ATF7IP2	GRHPR	TUBB1
ACSL1	C5	GATM	NIPSNAP1	SHMT1		BCO2	GSTZ1	UROC1
ACY1	C6	GC	NIT2	SHMT2		C4BPA	GSY2	ZNF281
ADH1A	CD302	GCHFR	OIT3	SLC10A1		C4BPB	HAGH	
ADH6	CDO1	GGH	ORM1	SLC13A5		CCL16	HAMP	
ADK	CFH	GSTO1	OTC	SLC22A7		CD5L	HLF	
AFF4	CFI	HABP2	PAH	SLC22A9		CDC37L1	HPS3	
AFM	CIDEB	HMGCL	PCBD1	SLC25A13		CES1	HSD11B1	
AGTR1	CLDN1	HMGCS2	PCCB	SLC27A2		CES2	IBTK	
AGXT	CPB2	HNF4A	PCK2	SLC2A2		CFP	IGFALS	
AGXT2	CPN1	HP	PEBP1	SLC30A1		CLEC4M	ITIH4	
AHSG	CPN2	HPD	PECR	SLC35D1		COLEC11	KMO	
AIG1	CPS1	HPN	PEMT	SLC38A3		CP	LARP4	
AKR1A1	CREB3L3	HPX	PGRMC1	SLC38A4		CRP	LECT2	
AKR1D1	CRYL1	HRSP12	PHYH	SLC39A14		CTH	LPIN2	
ALAS1	CYB5A	HSD17B4	PIPOX	SLC41A2		CYP1A2	MAMDC4	
ALB	CYP3A7	HSD3B7	PKLR	SLC43A1		CYP26A1	MASP1	
ALDH6A1	CYP4A11	HSPE1	PLA2G12B	SLCO2B1		CYP2A6	MASP2	
ALDH8A1	CYP4V2	ID2	PLG	SORD		CYP2B7P1	MBL2	
ALDOB	CYP8B1	IGFBP1	PNPLA3	SPRYD4		CYP2C8	MCL1	
AMBP	DCXR	IL1RAP	PRAP1	ST6GAL1		CYP2D6	MTHFD1	
ANG	DDT	INHBE	PRDX4	SULT2A1		CYP2E1	MYO1B	
ANGPTL3	DECR1	INSIG1	PROC	TAT		CYP39A1	N4BP2L1	
APOA1	EPHX1	ITIH1	PROS1	TDO2		CYP4A22	PHLDA1	
APOA2	ETFB	ITIH2	PROX1	TFR2		DEFB123	PLGLB2	
APOB	F10	KHK	PROZ	TM4SF4		DEPDC7	PON1	
APOC2	F13B	KLB	PXMP2	TM4SF5		DHRS1	PON3	
APOC3	F2	KLKB1	RBP4	TMEM176A		DMGDH	PPAPDC2	
APOE	F5	KNG1	RCL1	TMEM176B		ERRFI1	PZP	
APOH	F7	LASS2	SAA4	TMEM56		ETFDH	RTP3	
APOM	F9	LBP	SC5DL	TMPRSS6		FAM167B	SCUBE3	
ARG1	FAM96A	LCAT	SCP2	TP53INP1		FMO3	SDS	